

Direct Evidence of Controlled Structure Reorganization in a Nanoorganized Polypeptide Multilayer Thin Film

Zheng-liang Zhi and Donald T. Haynie*

Biomedical Engineering and Physics, Center for Applied Physics Studies, Louisiana Tech University,
PO Box 10348, Ruston, Louisiana 71272

Received May 3, 2004; Revised Manuscript Received July 29, 2004

ABSTRACT: Aspects of poly(L-lysine) (PLL) and poly(L-glutamic acid) (PLGA) multilayer thin film assembly, physical properties of the films, and changes in film structure on pH shift have been studied by far-UV circular dichroism spectroscopy (CD), ultraviolet spectroscopy (UVS), ellipsometry, quartz crystal microbalance (QCM), and atomic force microscopy (AFM). We show that CD can be used to assess the secondary structure content of a polypeptide multilayer film deposited on quartz substrates by electrostatic layer-by-layer assembly (LbL). Measurements have revealed that, under conditions where PLL and PLGA displayed a random coil-like conformation in solution, the polypeptides formed predominantly β -sheet structures in multilayer films fabricated by LbL. A substantial conformational change occurred on exposure of such films to a strongly acidic ($\text{pH} \leq 2.5$) or strongly basic ($\text{pH} \geq 12.0$) aqueous medium, from β -sheet to predominantly α -helical structure. pH shift thus may be a useful postpreparation approach for stimuli-responsive modification of the surface roughness, porosity, and permeability of preassembled polypeptide films or structures made from such films, e.g., microcapsules.

Introduction

LbL is a powerful tool for the preparation of multilayer thin films from various substances on virtually any substrate. The “building blocks” are alternating layers of oppositely charged chemical species, often polyelectrolytes, which can be deposited in a predetermined sequence. Under some conditions the film growth step can be as small as ~ 1 nm. Physical properties of an assembled film, for example layer thickness, film strength, and rigidity, will often depend on external conditions, notably ionic strength,^{1–3} pH,^{3–7} and temperature⁸ of the solutions in which the adsorbing polymers are dissolved. A change in the pH of solution, for instance, can affect the distribution of conformations of the dissolved polymers, their rigidity, and their assembly behavior.³ At the same time, LbL is generally understood to result in layered structures that are locally amorphous. Studies have shown, however, that a range of combinations of biopolymer exhibiting locally ordered structure can be incorporated into a thin film by LbL, for instance proteins,^{9,10} α -helical polypeptides,¹¹ and helical double-stranded DNA.^{12,13}

The structure and morphology of a polyelectrolyte multilayer can be modified by postpreparation treatment. For example, immersion of a multilayer structure in a solution of different ionic strength can form or break salt bridges between layers, swelling the structure in high salt or contracting it in low salt, and brief immersion of a film into a low- or high-pH solution can modify its porosity and permeability.^{14,15} This will be especially pertinent to thin films composed of “weak” polyelectrolytes, for example poly(acrylic acid) and poly(allylamine)^{16–19} and PLL and PLGA, as charge density depends strongly on pH. Such changes in structure can be ascribed to interchain anion–cation bond breakage and re-formation and related changes in polymer configuration.¹⁶ Direct and detailed evidence of changes in

polymer structure in a multilayer thin film, however, has proved more elusive.

Both the design of the overall structure and details of the constituent polymers will determine bulk properties of a thin film prepared by LbL. Approaches used to ascertain internal structural features of a film, for example average layer thickness, roughness of internal interfaces, and material density, include neutron and X-ray reflectivity^{20–22} and X-ray photoelectron spectroscopy.^{6,23,24} Use of these techniques, however, is difficult and time-consuming. There thus is a need for a relatively simple, low-cost, and rapid means of determining the global structural properties of polyelectrolytes in a multilayer film. Only a few such approaches are available. Infrared spectroscopy (IR) has typically been used to investigate polyelectrolytes in multilayer films,^{4,5} including polypeptides.^{25–27} Quantification of polypeptide secondary structure based on IR spectroscopic information, however, is frustrated by the extensive overlap of absorption bands resulting from variations in intra- and intermolecular interactions and band coupling^{28–30} and thus is not particularly sensitive to secondary structure content. This can complicate the monitoring of film assembly involving proteins or polypeptides, particularly if any of the adsorbing species has an IR adsorption band resembling the amide I band of the peptide bond.

CD, a moderate-resolution but highly informative technique that can reveal structural information on chiral molecules, would appear to be a useful alternative to study of molecular structure in thin films. The method has been used successfully and extensively to determine the conformation of proteins and polypeptides in solution.^{3,31–33} CD has also been used to study the chirality of molecular films involving a chiral anionic dye,^{34,35} grafted PLL and PLGA films,³⁶ and adsorbed proteins.³⁷ In the present work we demonstrate use of CD to characterize the secondary structure content of polypeptides in multilayer thin films fabricated by LbL. The approach enables a moderately accurate determination of the three basic classes of structure of polypep-

* Corresponding author: e-mail haynie@latech.edu; Tel +1 318 257 3790; Fax +1 318 257 2562.

tides, viz. α -helix, β -sheet (and β -turn), and random coil. To the best of our knowledge, CD has not previously been applied to the structural characterization of multilayer thin film prepared from disordered polypeptides.

We chose PLL and PLGA for this study because they are optically active and therefore suitable for CD analysis, and they are readily available from commercial sources. In previous work, we studied how the solution structure of PLL and PLGA correlates with multilayer film assembly behavior.³ PLL–PLGA-based films are known to have potential for biomaterials applications such as biosensors, biocoatings for cellular adhesion, and microcapsules for drug delivery. In the present work, we have characterized pH-induced changes in conformation and morphology in LbL multilayer films of PLL and PLGA using QCM, absorption spectroscopy, ellipsometry, and AFM, and interpreted changes in secondary structure under different conditions in terms of film porosity. The data show that PLGA can undergo a rapid transition from β -sheet to α -helix in a nanoorganized PLL–PLGA multilayer thin film on exposure to a strongly acidic or basic aqueous medium. This structural change occurs on a time scale of minutes, and it will ordinarily be accompanied by some film deterioration and, apparently, increased film surface roughness and porosity.

Experimental Methods

Materials. PLGA sodium salt (MW 84.6 kDa, MALLS MW 53.8 kDa) and PLL hydrobromide salt (MW 84.0 kDa, MALLS MW 94.6 kDa), both in lyophilized form, were from Sigma and used without further purification. LbL experiments were done at pH 7.4 in 10 mM tris(hydroxymethyl)aminomethane (Tris)–HCl buffer and 0.15 M NaCl. Under such conditions, which resemble those of a physiological medium, PLL (a polycation of 1 amino group per monomer, pK_a 10.5) and PLGA (a polyanion of 1 carboxyl group per monomer, pK_a 4.2) are effectively fully ionized; the linear charge density is close to 1 charge per monomer at neutral pH.

Quartz microscope slides for CD and UVS measurements were from Electron Microscopy Sciences, and glass microscope slides for AFM measurements were from Chase Scientific Glass. The 75×25 mm² substrates were cut into rectangles of 10×25 mm², cleaned for 30 min in 1% SDS at 80 °C with agitation, washed with 1% NaOH in ethanol–H₂O (60/40, v/v), rinsed extensively with ultrapure water (18.2 M Ω ·cm resistivity) (Milli-Q System, Millipore), and dried under a stream of gaseous N₂.

Silicon wafers (Si(100), 0.5 mm thick, 10.2 mm diameter), from Silicone Technology Corp., were cut into rectangular plates of 1.5×1 cm² for ellipsometry measurements. (*Caution:* SiO₂/Si reacts slowly with alkaline. Avoid the use of alkaline cleaning agents to treat Si substrates for an extended period of time or to assemble films.) The Si substrates were cleaned and oxidized/hydrophilized by immersion for 30 min in a hot 1:3 (v/v) mixture of 98% H₂SO₄ and 27% H₂O₂, then rinsed extensively with ultrapure water, and blown dry with a stream of gaseous N₂. (*Caution:* This cleaning solution, known as piranha, is strongly oxidizing. It reacts violently with organic substances and should not be stored in a closed container.)

Multilayer Deposition. PLL–PLGA multilayer films were fabricated on negatively charged quartz, glass, oxidized silicon plates, and QCM quartz resonators by consecutive immersion of the substrates for 20 min in 1 mg/mL PLL or 1 mg/mL PLGA in aqueous solution. The substrate was retracted and rinsed thrice with ultrapure water between each deposition step and after the final step. In each adsorption cycle a bilayer film of PLL–PLGA was formed on both sides of the plate. After a desired number of layers were deposited, the substrate-supported films were dried at room temperature under a stream of gaseous N₂.

To investigate changes in polypeptide conformation, a series of acidic (pH 1.5–4.0) and basic (pH 9.0–13.0) solutions were prepared by addition of either 5 M HCl or 2 M NaOH to an aqueous solution of 150 mM NaCl. Multilayers adsorbed onto a substrate were immersed into one of these solutions for ca. 10 min, rinsed with ultrapure water for 20–30 s, and blown dry with gaseous N₂. Following measurement, the film was again immersed for 30 min in 10 mM Tris, 0.15 M NaCl, pH 7.4, rinsed with ultrapure water, and dried with N₂. The resulting films were used for studies of pH-induced changes in film properties.

Film Characterization. CD spectra in the wavelength range 180–260 nm were recorded using a Jasco model J-810 spectropolarimeter (Japan) and used to characterize the secondary structure content of polypeptide multilayer thin films deposited on quartz. To record a film spectrum, a slide substrate was fixed to a CD cell support with an adhesive film and positioned in the cell holder in the sample compartment. The area of the beam passing through the film (~ 80 mm²) was constant. The CD instrument was set at 100 mdeg sensitivity, 1 nm bandwidth, 1 s response time, 1 nm data pitch, and 100 nm min^{−1} scan rate. 20–30 scans were accumulated and averaged in each case. The measured ellipticity values recorded in mdeg could not be normalized for path length or polymer concentration. This does not diminish the ability of the technique to determine the structure of the polypeptides, however, as such information depends only on the shape of spectrum, not its magnitude at any given wavelength. Baseline spectra were collected by measuring the CD signal of the quartz substrate prior to film assembly. Final spectra were obtained by subtracting the baseline spectrum from the corresponding sample spectra. Decoupling of the far-UV CD spectra into contributions from α -helix, β -sheet, β -turn, and random coil was done using the CD Pro software suite (program CONTINIL).³⁸

AFM images of PLL–PLGA multilayer thin films deposited on glass plates were obtained in air with a Quesant Instrument Corp. Q-Scope 250 AFM operating in noncontact mode. NSC 16 cantilevers with silicon nitride tips were used throughout.

The optical thickness of PLL–PLGA thin films deposited on the polished face of oxidized silicon plates was measured using a Sentech Instruments GmbH SE 850 ellipsometer (Germany) operating in the wavelength range 350–820 nm at 70° incident angle. Both film thickness and refractive index were determined by nonlinear least-squares regression. Each polypeptide multilayer thin film assembled on a 10×15 mm silicon plate was assumed to be approximately homogeneous in the fitting procedure.

QCM (Agilent 53131A 225 MHz universal counter) and silver-coated resonators (Sanwa Tsusho Co., Japan) were used to monitor the stepwise growth of polypeptide multilayer films and stability in solution. Each resonator was composed of a thin circular quartz plate ca. 0.15 mm thick and ca. 8.3 mm in diameter, with both faces patterned and sputter-coated with silver electrodes. The resonator was excited at its fundamental frequency (ca. 9 MHz). Change in resonant frequency of the quartz crystal, Δf , was assumed proportional to the deposited mass increment resulting from adsorption of material.³⁹ Frequency shift is related to mass increment as $-\Delta f = \Delta m(1.83 \times 10^8)/A$, where the resonator surface area $A \approx 0.16$ cm². In time-course experiments on mass loss from a film, a resonator with 10 deposited layers of polypeptide was dipped into a strongly acidic solution (pH 2.0) or a strongly alkaline solution (pH 12.0) for a defined period of time (5 min–24 h). The measured value of $-\Delta f$ was plotted against exposure time.

Absorption spectra of multilayers deposited on a quartz substrate were recorded in the wavelength range 190–300 nm using a Shimadzu UV-1650 PC UV–vis spectrophotometer (Japan). Polypeptide films were assembled at neutral pH, exposed to an acidic or alkaline solution, and then exposed again to a neutral pH solution. The “optical mass” of thin films assembled on quartz was monitored by UVS at each stage of the treatment process. It was assumed that the absorption coefficient of the polyelectrolytes at 221 nm was approximately independent of conformation.⁴⁰

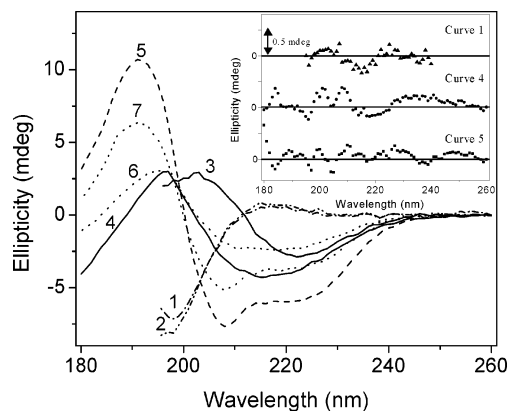


Figure 1. CD spectra of PLL and PLGA in solution and in a multilayer thin film: (1) 0.05 mg/mL PLL in aqueous solution at pH 7.4 (10 mM Tris buffer with 0.15 M NaCl); (2) 0.05 mg/mL PLGA in aqueous solution at pH 7.4; (3) 0.1 mg/mL PLL–PLGA complex in aqueous solution at pH 7.4; (4) PLL–PLGA multilayer composed of 10 layers deposited onto a quartz plate from an aqueous solution at pH 7.4; (5) multilayer after treatment at pH 2.0 for 10 min; (6) multilayer after subsequent immersion in a solution at pH 7.4 for 30 min after pH 2.0; (7) multilayer after subsequent immersion in a solution at pH 2.0 for 10 min following measurement of curve 6. Curves 1–3 were not measured below 197 nm to avoid damaging the photomultiplier. The inset shows the residues from deconvolution analysis as a function of wavelength. Note the change in scale of the vertical axis. Curves 1, 4, and 5 were chosen as representative examples of secondary structure content. Root mean square deviation was 0.15, 0.22, and 0.50 mdeg for spectrum 1, 4, and 5, respectively.

Results

CD. Figure 1 shows typical CD spectra of PLL, PLGA, and PLL–PLGA complexes in aqueous solution at pH 7.4 or in a multilayer thin film fabricated on a quartz substrate at the same pH. The inset shows the residuals from deconvolution analysis of representative spectra. Spectra of the polypeptides in solution (curves 1 and 2) show a slight positive π – π^* transition at ca. 216 nm and a strong negative n – π^* transition at ca. 198 nm, indicating random coil-like structure. The spectrum of the PLL–PLGA complex in solution (curve 3) displays a negative π – π^* transition at ca. 222 nm and a positive n – π^* one at ca. 202 nm, suggesting β -sheet structure. Similarly, the β -sheet-like spectrum of a PLL–PLGA multilayer thin film (curve 4) displays a negative π – π^* transition at ca. 216 nm and a positive n – π^* one at ca. 197 nm.

When PLL–PLGA films fabricated at pH 7.4 were exposed to aqueous solution at pH 2.0, the CD spectrum changed dramatically. The result (curve 5) was a strong positive (π – π^*)_{perpendicular} band at 191 nm, a negative (π – π^*)_{parallel} band at 208 nm, and negative n – π^* band at 222 nm, indicating α -helix-like structure. Analysis of time course revealed that this structural transformation took place on a time scale of 5–10 min; further immersion of the film in acidic solution for up to 2 days did not substantially affect the shape of the CD spectrum (data not shown).

Reversibility of the pH-induced structural transformation was tested by immersing the acidic pH-treated PLL–PLGA thin films in 10 mM Tris, 0.15 M NaCl, pH 7.4 for 30 min. The CD spectrum recorded after such treatment (curve 6) is broadly similar to curve 4. No further change in the spectrum was observed when the time of exposure to neutral-pH solution was extended to 24 h. The reversibility of the pH-induced structural

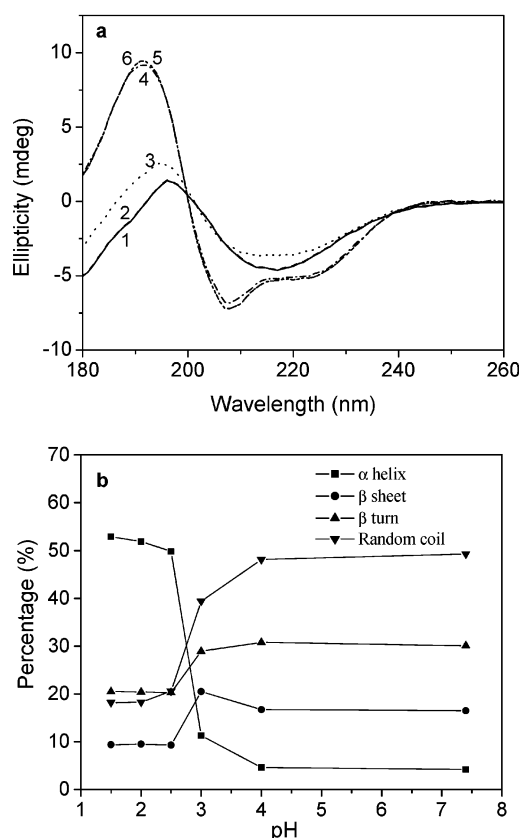


Figure 2. Structural changes in a PLL–PLGA multilayer film in the acidic pH range. (a) Spectra of a 10-layer film deposited on a quartz plate at pH 7.4: (1) before pH shift; (2) pH 4.0; (3) pH 3.0; (4) pH 2.5; (5) pH 2.0; (6) pH 1.5. (b) Deconvolution results. Content of different secondary structures is shown as a function of pH.

transformation was further tested by reimmersion the neutral pH-treated PLL–PLGA thin films in HCl aqueous solution at pH 2.0 for 10 min. The CD spectrum recorded after such acidic treatment, shown in Figure 1 as curve 7, is similar to curve 5 but with some decrease in amplitude.

The pH dependence of the polypeptide multilayer film CD spectrum was studied in further detail in the range 1.5–7.4. As shown in Figure 2a, the shape of the spectrum was virtually independent of pH in the range 4.0–7.4 (curves 1 and 2). A dramatic shift occurred, however, as the pH was decreased to ca. pH 2.5 (curves 3 and 4), but no further change was found on reducing the pH to 1.5 (curves 5 and 6). Deconvolution of the spectra gave the secondary content values shown in Figure 2b. Changes in film structure were also studied at basic pH, as shown in Figure 3a. This treatment resulted in a significant decrease in the CD signal. The secondary structure content at basic pH revealed by spectral deconvolution is shown in Figure 3b. To determine the origin of the observed effects, complementary experimental data were sought using UVS and QCM as described below. The CD spectrum of a single layer of PLL and of a single bilayer of PLL–PLGA on a quartz substrate were collected and analyzed. In both cases, however, the CD signal was too weak to assess the effect of pH on polypeptide structure in the film, even after hundreds of scans (Balkundi, S.; Haynie, D. T., unpublished data).

UVS. UV absorbance of polypeptide multilayers deposited on quartz was measured to assess changes in

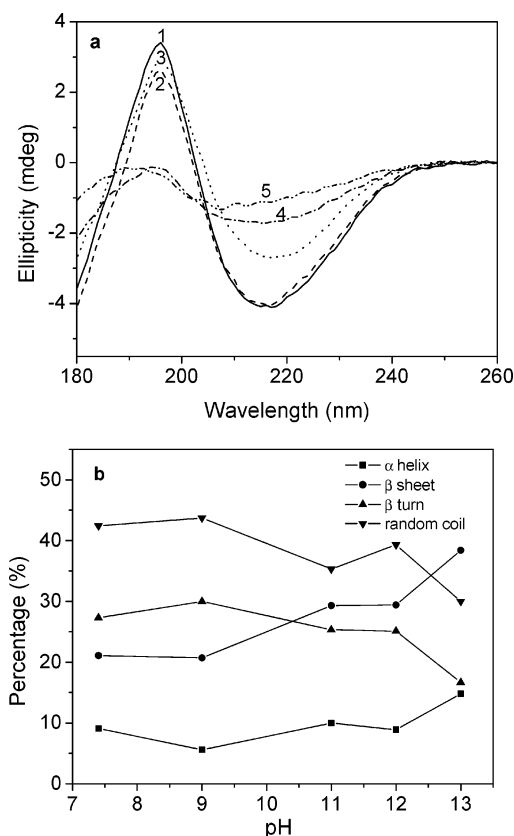


Figure 3. Structural changes in a PLL-PLGA multilayer film in the basic pH range. (a) Spectra of a 10-layer film deposited on a quartz plate at pH 7.4: (1) before pH shift; (2) pH 9.0; (3) pH 11.0; (4) pH 12.0; (5) pH 13.0. (b) Deconvolution results. Content of different secondary structures is shown as a function pH.

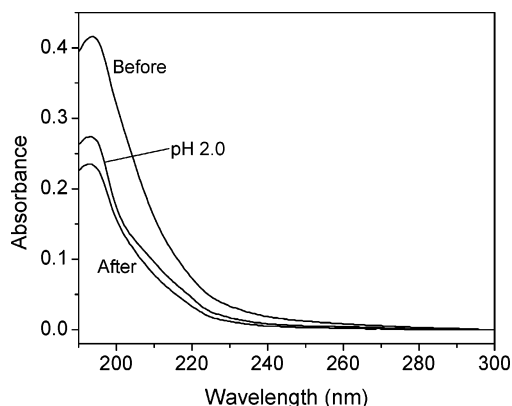


Figure 4. UVS monitoring of the absorbance of a PLL-PLGA multilayer thin film deposited at pH 7.4 on a quartz plate before and after exposure to a strongly acidic (pH 2.0) solution for 10 min and after subsequent exposure to 10 mM Tris buffer at pH 7.4 for 30 min.

optical mass during the acidic- and alkaline-treatment experiments described above. UV spectra of 11-layer-thick PLL-PLGA films (innermost and outermost layers, PLL) at different stages of treatment are shown in Figure 4. About 35% of initial signal intensity ("before") was lost on treatment with strongly acidic solution in the first 10 min of exposure, similar to the CD result discussed above. Increasing the immersion time (up to 48 h) at pH 2 resulted in virtually no additional change in the UV absorption spectrum (data not shown). Following exposure to acidic pH, films were immersed in a buffered solution at pH 7.4. Signal intensity ("after")

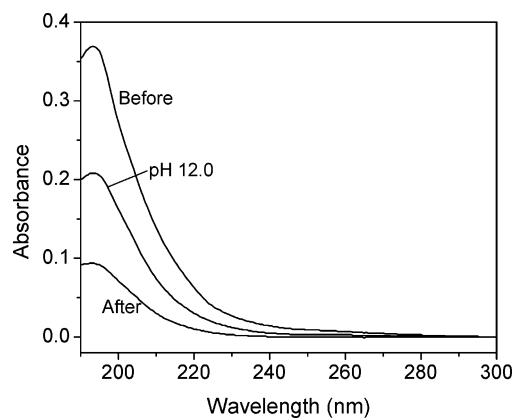


Figure 5. UVS monitoring of the absorbance of a PLL-PLGA multilayer thin film deposited at pH 7.4 on a quartz plate before and after exposure to a strongly basic (pH 12.0) solution for 10 min and after subsequent exposure to 10 mM Tris buffer at pH 7.4 for 30 min.

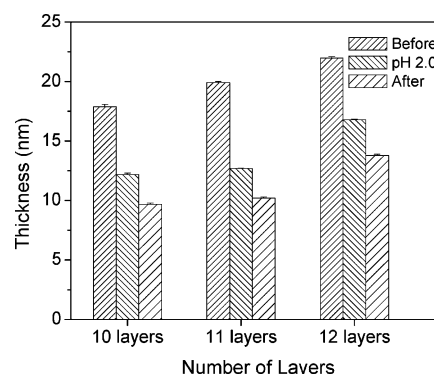


Figure 6. Thickness of 10, 11, or 12 layers of PLL-PLGA deposited at pH 7.4 on oxidized silicone plates, as determined by ellipsometry. Bars represent thickness before and after exposure to a strongly acidic (pH 2.0) solution for 10 min and after subsequent exposure to 10 mM Tris buffer at pH 7.4 for 30 min.

was found to have decreased further, by as much as 6%. Optical mass loss was also studied under strongly basic conditions, as shown in Figure 5. The initial UV signal intensity ("before") diminished even more after such treatment than at acidic pH (45% vs 35%). Exposure of a film to a neutral solution following treatment at pH 12 resulted in an additional 30% decrease in signal intensity ("after"), substantially more than after treatment at pH 2.

Ellipsometry. Dried multilayer films of PLL and PLGA on an oxidized silicone substrate were studied by ellipsometry to determine film thickness. The approach was also used to assess the effect of film exposure to a strongly acidic or strongly basic environment. Figure 6 gives the measured thickness of films of 10, 11, or 12 layers, assembled at neutral pH and room temperature and treated as indicated. The thickness of one layer of PLL deposited as the 11th layer was 2.0 nm, while that of PLGA deposited as the 12th layer was 2.1 nm. The average thickness per layer of a 12-layer PLL-PLGA film was 1.8 nm. On immersion of a film in a solution at pH 2.0 for 10 min, the overall thickness decreased by 28%. Subsequent immersion of the film in a solution at pH 7.4 resulted in a further decrease in thickness, to a total loss of 41%. Corresponding experiments could not be done under alkaline conditions because of instability of the silicone substrate.

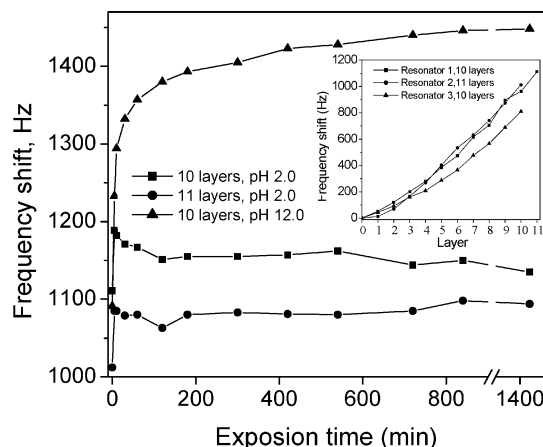


Figure 7. QCM monitoring of mass changes of PLL-PLGA multilayer thin films. The films were deposited at pH 7.4 on a quartz resonator (inset) and exposed to a strongly acidic solution (pH 2.0) or a strongly basic solution (pH 12.0). Even numbers represent adsorption of PLGA and odd numbers adsorption of PLL. For acidic pH, films of 10 and of 11 layers were examined to test the possible significance of film surface charge. For alkaline pH, only a film of 10 layers was tested.

QCM. This method was used to monitor both changes in adsorbed material during multilayer film assembly on quartz resonators and the stability of the PLL-PLGA thin films in solution. The frequency shift varied nonlinearly with adsorption cycle during assembly (Figure 7, inset). Films of 10 layers (PLGA outermost) and 11 layers (PLL outermost) showed frequency increase on exposure to pH 2.0 for 5 min of 8% and 7.3%, respectively. In both cases, the resonant frequency remained stable or decreased slightly when the exposure time was extended to 24 h. By contrast, film exposure to an alkaline solution at pH 12.0 resulted in a continuous increase in QCM signal of up to 32% over a 24 h exposure period, indicating a substantial loss of material from the resonator.

AFM. Figure 8 shows AFM images for a typical 10-layer PLL-PLGA film before and after exposure to pH 2.0 solution and after return to pH 7.4. In general, the surface roughness of the films had a lateral periodicity that varied with pH, as seen in the surface profiles. The average peak height of the sample in (a) was less than 3 nm, and the average distance between the peaks is 90 nm. On exposure to acidic solution, the average peak height increased to 5 nm, and the average distance between peaks increased to 195 nm (b). The structure of the film exhibited further rearrangement on return to pH 7.4 (c): the average peak height was less than 3.5 nm, and the distance between peaks was ca. 70 nm.

Discussion

The most significant results of this work concern secondary structure content of PLL-PLGA multilayer films, changes in film structure on exposure to extreme pH, and the surface roughness and apparent porosity of the films. Morphological changes of polyelectrolyte multilayers resulting from a change in pH or salt concentration have been reported for multilayers of nonbiocompatible polyelectrolytes.^{15–19} None of the reports, however, deal with the microscopic changes in polymer structure that must underlie the observed macroscopic changes in film properties. Moreover, earlier reports on polypeptide secondary structure in films, assessed by Fourier transform (FT)-IR,^{25–27} needed to be reevaluated for reasons given above.

Secondary Structure Content of PLL-PLGA Multilayer Films. The polypeptide backbone absorbs light at wavelengths below 240 nm. Left- and right-circularly polarized beams of light are absorbed to a different extent, the amount depending on polypeptide conformation. A polypeptide is a chiral molecule. CD thus is useful for determining global structural features of polypeptides and particularly well-suited for monitoring changes in molecular structure upon perturbation. CD has commonly been employed to study secondary structure content of peptides and proteins in aqueous

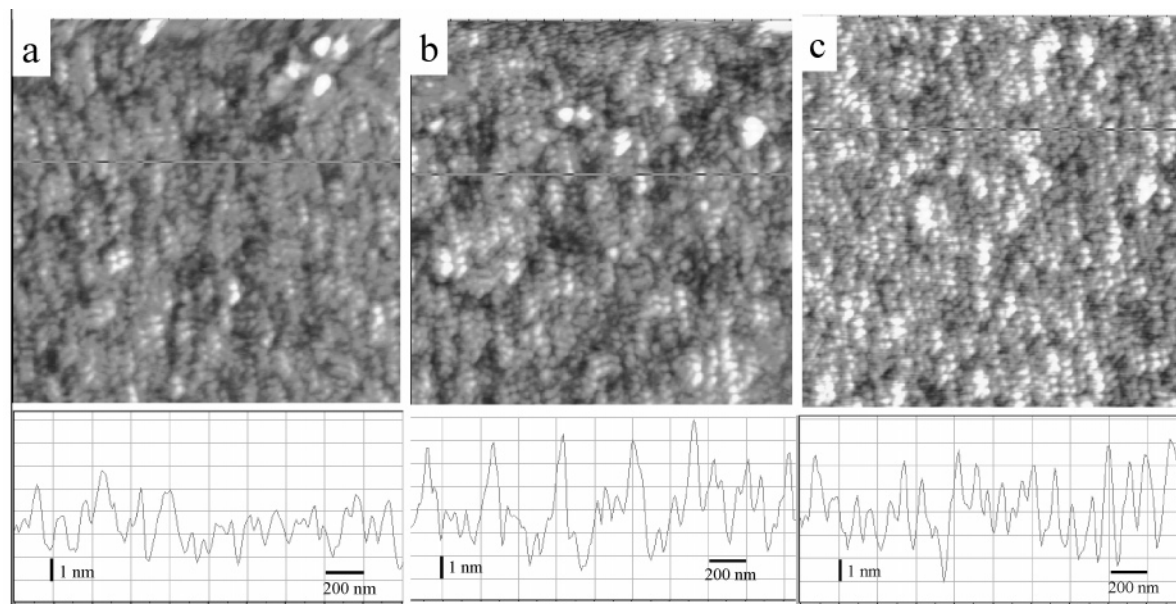


Figure 8. AFM analysis of a 10-layer PLL-PLGA multilayer thin film on a glass substrate: upper panels, height mode images; lower panels, profilometric sections of the indicated locations. Different stages during the exposure process are shown: (a) as-prepared, (b) after exposure to a pH 2.0 solution for 10 min, and (c) after subsequent return to pH 7.4. Image dimensions are $2 \times 2 \mu\text{m}^2$, and the z -axis scales are 10 nm for (a) and (c) and 12 nm for (b). The average peak-to-peak distances are (a) 90 ± 17 nm, (b) 194 ± 34 nm, and (c) 69 ± 14 nm ($n = 10$). The surface roughness of the glass substrates was typically less than 2 nm.

Table 1. Percentage Secondary Structure Content of PLGA and PLL in Solution and in Multilayer Thin Films; Values Were Obtained by Deconvolution of CD Spectra in Figure 1

	percentage secondary structure			
	α -helix	β -sheet	β -turn	coil
PLGA in solution, pH 7.4	6.8	35.2	18.8	39.2
PLL in solution, pH 7.4	5.9	29.4	20.2	44.5
PLGA–PLL complex in solution, pH 7.4	4.8	48.5	19.3	27.4
PLGA–PLL film, before ^a	4.9	19.6	30.7	44.7
PLGA–PLL film, pH 2.0 ^b	59.7	4.0	17.7	18.9
PLGA–PLL film, after ^c	18.7	29.0	23.9	28.3
PLGA–PLL film, pH 2.0 again ^d	39.4	13.3	22.4	24.8

^a As-prepared at pH 7.4. ^b After exposure to pH 2.0 for 10 min. ^c After subsequent exposure to pH 7.4 for 30 min. ^d After a second exposure to pH 2.0 for 10 min.

solution, for example in protein folding research.^{41–43} Characteristic CD signatures of the three major classes of peptide secondary structure, viz. α -helix, β -sheet, and random coil, are well-known⁴⁴ and form the basis of spectral deconvolution.³⁸

The CD spectra of PLL and PLGA in solution (curves 1 and 2 in Figure 1) suggest random coil-like structure. This is similar to previous reports in the scientific literature^{45,46} and corroborated by deconvolution (Table 1). By contrast, the spectra of a PLL–PLGA complex in aqueous solution (curve 3) and of a dehydrated PLL–PLGA multilayer thin film (curve 4) are strongly suggestive of β -sheet structure. The data thus indicate the formation of β sheet, both on soluble complexation and on polypeptide adsorption; the structures are markedly different from those of the pure peptides in solution. A 5–6 nm blue shift of the negative and positive Cotton effects resulted from formation of the PLL–PLGA multilayer. Deconvolution of the CD spectra suggests that the PLL–PLGA complex in solution had a somewhat higher β -sheet content (68%) and lower coil-like content (27%) than the corresponding multilayer (50% β -sheet and 45% coil-like), owing perhaps to interaction between polymers in different layers and with the quartz substrate. While polymer adsorption has a time scale of minutes,⁴⁷ the kinetic process of β -sheet structure formation in the film might be markedly slower, even if changes in polypeptide multilayer structure can occur on a time scale of minutes. Researchers who have used FT-IR to study polypeptide structure in multilayers have reported that the secondary structure content of PLL–PLGA in the multilayer was very close to that in the soluble complex (β -sheet 45–48%, α -helix 18%).^{26,27} Comparison of the raw spectra of FT-IR and of CD thus has revealed that CD is probably better-suited than FT-IR to determination of polypeptide secondary structure in solution and probably also in thin films.

The pH-dependent driving force for conformational change in a polypeptide chain appears to be inversely related to the linear charge density of the polymer. Protonation of COO[−] groups in PLGA and deprotonation of NH₃⁺ groups in PLL in a highly acidic or highly basic environment, respectively, will neutralize the charge on the polypeptide chain, whether the polymer is in solution or in a film. Consequences of this will include severing of interchain ionic interactions and, in some cases, large-scale reorganization of secondary structure. For example, PLGA in aqueous solution is known to exhibit a dramatic conformational change, from a

random coil-like state to a helical state, on pH shift from neutral to near or below the pK_a of glutamic acid (ca. 4.2); qualitatively, the same behavior is exhibited by PLL on a change of pH from neutral to near or higher the pK_a of lysine (ca. 10.5).³

In the present work we have found that the behavior of PLGA in a PLL–PLGA multilayer film resembles its solution properties, despite presumably extensive interpenetration of polymers from adjacent layers and strong ionic interactions between interlayer β -sheets. The shape and signal intensity of the CD spectrum of the PLL–PLGA multilayer film were virtually constant in the range pH 4–7. As the acidity of environment increased to pH 3.0, the film gradually became more helical (Figure 2a). Some of the film polypeptides, presumably PLGA, underwent a change in conformation in this process from β -sheet to α -helix (Figure 2b and Table 1). The midpoint of the structural transition occurred at ca. pH 2.9 (Figure 2b), about 1.3 pH units lower than the pK_a of glutamic acid in aqueous solution. Similarly at basic pH, the optimal pH value for structural rearrangement of a PLL–PLGA multilayer was above 12, compared to a pK_a of 10.5 for lysine in aqueous solution (Figure 3a,b).

As shown in Table 1, deconvolution suggests that the PLL–PLGA films fabricated at pH 7.4 had a significant content of β -sheet structure (ca. 50%) and relatively little α -helix (ca. 5%). Upon exposure to pH 2.0, however, many of the polypeptides in the film became α -helical (ca. 60%); the percentage of β -sheet and random coil-like structure declined significantly. Return to neutral pH of the film thus treated resulted in a substantial decrease in α -helix and an increase in β -sheet content. Return of the neutral pH-treated PLL–PLGA thin film to pH 2.0, again for 10 min, resulted in many of the polypeptides in the film becoming α -helical (39.4%), as before. Thus, changes in molecular structure within a film were largely reversible. Such changes and reversibility of structure were less significant at basic pH (Figure 3b) than at acidic pH (Figure 2b).

These data are consistent with independent reports in which the pK_a of COOH/COO[−] shifted to ca. 2.5 in a weak polyelectrolyte multilayer film from 4.2 in aqueous solution.^{16,48} The pK_a shift in the present work thus can be interpreted as the dissociation constants of side chains in PLL or PLGA being substantially affected by the presence of the oppositely charged polyion in the film; PLGA is a weak polyacid. It would appear that PLGA becomes a stronger polyacid (has a lower pK_a) and PLL becomes a stronger base (has a higher pK_a) on being embedded in a PLL–PLGA multilayer film.

Stability of PLL–PLGA Multilayer Films on Exposure to Extreme pH. CD spectra indicate that, on immersing a pH 2-treated multilayer film in neutral solution (pH 7.4), a large proportion of the molecules returned to β -sheet structure; substantial reversibility of pH-induced structural change was found to occur. Some mass was lost, however, during structure reorganization at acidic pH, as indicated by photomultiplier voltage recorded in a second channel during CD experiments (data not shown). About 35% of material in the film was lost on treatment with a strongly acidic solution (pH 2.0), and most of the mass loss was found to occur within the first 10 min of exposure, as observed by UVS. Such mass loss presumably was due to partial dissociation of polypeptide complexes in films during structure reorganization.

The ellipsometry measurements show that PLL–PLGA film thickness decreased by 28% on immersion for 10 min in a solution at pH 2.0. Again, the cause of film disintegration was presumably structure reorganization resulting from protonation of carboxylate groups in PLGA. The extent of change in film thickness on exposure to acid pH is in good agreement with that determined by UVS.

The shift in frequency on a QCM resonator varied nonlinearly with each adsorption cycle during polypeptide assembly (Figure 4, inset), similar to previous reports.^{3,49,50} PLL–PLGA films of 10 layers (PLGA outermost) and 11 layers (PLL outermost) showed an 8% and 7.3% increase in resonant frequency, respectively, on exposure to pH 2.0 for 5 min. This suggests that mass loss during polymer structure reorganization was approximately independent of the character of the outermost layer. The resonant frequency remained more or less stable during the prolonged exposure time (up to 24 h) at pH 2.0, suggesting that loss of mass occurred during film structure reorganization and that the reorganized thin film remained stable under low-pH conditions. Substantial loss of material from weak polyelectrolyte multilayers at high pH has previously been reported and interpreted as film delamination, resulting from deprotonation of amine groups and development of charge imbalance in the film.¹⁷

Comparison with the results of UVS and ellipsometry suggests that QCM data on loss of material from films may be somewhat underestimated. Less loss of material may result from interactions not present on SiO₂ substrates. Such interactions may be significant for inhibiting the loss of material at strongly acidic pH, where PLGA will ordinarily lose most of its charge if not all of it.

Surface Roughness and Porosity of PLL–PLGA Multilayer Films. AFM shows that films assembled at pH 7.4 were relatively smooth and compact. A previous report had shown that the surface roughness of polyelectrolyte multilayers was on the order of 1 nm and independent of the number of layers adsorbed.¹⁵ The present work would suggest that the roughness of an untreated film was due mainly to the surface of the substrate, which typically will have a roughness of ca. 2 nm. The structural changes resulting from film immersion in acidic solution correspond to a significant increase in surface roughness and, possibly, formation of porous structure. This macroscopic change in film properties must be a result of microscopic changes in polymer structure. Reversibility of the structural change evident by CD was also seen by AFM. The decreased roughness and increased compactness observed on return to neutral pH would appear to correspond to a helix-to-sheet transition in the film.

In the fabrication of a multilayer structure by LbL, polyelectrolytes of the same charge will repel each other during the self-regulatory process of adsorption to achieve an organized layer of uniform thickness. This reverses the surface charge of the substrate. An oppositely charged polyelectrolyte can then adsorb onto the deposited layer, driven by electrostatic attraction. The formation of β -sheet assemblies in adjacent layers through interlayer hydrogen bonding promotes the organization of a uniform and, apparently, remarkably stable multilayer film. Upon exposure to extreme pH, however, some of the polypeptide chains will become partly if not fully discharged, leading to a corresponding

cleavage of interchain ionic bonds. Thermal fluctuations will be sufficient to break remaining weak interactions, e.g., hydrogen bonds, particularly if they are not as well organized as in proteins. Consequently, relatively large-scale reorganization of film structure will be possible, and more energetically favorable but less globally organized α -helices will be able to form. Such microscopic changes in structure will give rise to changes in macroscopic film properties, for example, porosity as observed in this study. Specific details of conditions can then be chosen to achieve the desired properties, for example, surface roughness and, presumably, porosity.

Conclusions

We have demonstrated the use of CD in determining the secondary structure content of LbL multilayer thin films of polypeptides, and we have used CD to monitor the pH-induced changes in polypeptide structure in such films. The data show that PLL–PLGA films assembled at neutral pH have a predominantly β -sheet character. The transformation of the secondary structure of the polypeptides in the film from β -sheet to α -helix would appear to result in a more open and loose film morphology. QCM, CD, and UVS studies of film stability have suggested that strongly acidic pH promotes the formation of pores in the polypeptide films. Such pH-induced changes could possibly be useful for altering the permeability of a preassembled thin film or creating a more desirable film porosity, for example, for control over cell adhesion to a substrate coated with a polypeptide multilayer film. Further studies will be directed to effects on secondary structure of change of assembly conditions, for example, ionic strength and pH. The ability to “tune” surface roughness or porosity in unsupported biocompatible films (e.g., in hollow capsules) could also be useful for applications in microencapsulation.

Acknowledgment. We thank Bingyun Li, Satish Bharadwaj, Prof. Robert Woody, an anonymous reviewer for helpful suggestions and Qun Gu for assistance with the AFM measurements. This research was supported by an enhancement grant from the Louisiana Space Consortium (Louisiana NASA EPS-CoR, Project R 127172) and the 2002 Capital Outlay Act 23 of the State of Louisiana (Governor’s Biotechnology Initiative).

References and Notes

- (1) Decher, G.; Schmitt, J. *Prog. Colloid Polym. Sci.* **1992**, *89*, 160–164.
- (2) Dubas, S. T.; Schlenoff, J. B. *Macromolecules* **2001**, *34*, 3736–3740.
- (3) Haynie, D. T.; Balkundi, S.; Palath, N.; Chakravarthula, K.; Dave, K. *Langmuir* **2004**, *20*, 4540–4547.
- (4) Shiratori, S. S.; Rubner, M. F. *Macromolecules* **2000**, *33*, 4213–4219.
- (5) Yoo, D.; Shiratori, S. S.; Rubner, M. F. *Macromolecules* **1998**, *31*, 4309–4318.
- (6) Phuvanartnuruks, V.; McCarthy, T. J. *Macromolecules* **1998**, *31*, 1906–1914.
- (7) Clark, S. L.; Hammond, P. T. *Langmuir* **2000**, *16*, 10206–10214.
- (8) Büscher, K.; Graf, K.; Ahrens, H.; Helm, C. A. *Langmuir* **2002**, *18*, 3585–3591.
- (9) Schwinte, P.; Voegel, J. C.; Picart, C.; Haikel, Y.; Schaaf, P.; Szalontai, B. J. *J. Phys. Chem. B* **2001**, *105*, 11906–11916.
- (10) Simonian, A. L.; Revzin, A.; Wild, J. R.; Elkind, J.; Pishko, M. V. *Anal. Chim. Acta* **2002**, *466*, 201–212.

- (11) Müller, M. *Biomacromolecules* **2001**, *2*, 262–269.
- (12) Sukhorukov, G. B.; Möhwald, H.; Decher, G.; Lvov, Y. M. *Thin Solid Films* **1996**, *284*, 220–223.
- (13) Montrel, M. M.; Sukhorukov, K. B.; Petrov, A. I.; Shabarchina, L. I.; Sukhorukov, B. I. *Sens. Actuators, B* **1997**, *42*, 225–231.
- (14) Dubas, S. T.; Schlenoff, J. B. *Langmuir* **2001**, *17*, 7725–7727.
- (15) Fery, A.; Schöler, B.; Cassagneau, T.; Caruso, F. *Langmuir* **2001**, *17*, 3779–3783.
- (16) Mendelsohn, J. D.; Barrett, C. J.; Chan, A. J.; Mayes, A. M.; Rubner, M. F. *Langmuir* **2000**, *16*, 5017–5023.
- (17) Harris, J. J.; Bruening, M. L. *Langmuir* **2000**, *16*, 2006–2013.
- (18) Hiller, J. A.; Mendelsohn, J. D.; Rubner, M. F. *Nature Mater.* **2002**, *1*, 59–63.
- (19) Hiller, J. A.; Rubner, M. F. *Macromolecules* **2003**, *36*, 4078–4083.
- (20) Schmitt, J.; Grünwald, T.; Decher, G.; Pershan, P. S.; Kjaer, K.; Lösche, M. *Macromolecules* **1993**, *26*, 7058–7063.
- (21) Lösche, M.; Schmitt, J.; Decher, G.; Bouwman, W. G.; Kjaer, K. *Macromolecules* **1998**, *31*, 8893–8906.
- (22) Phuvanartnuruks, V.; McCarthy, T. J. *Macromolecules* **1998**, *31*, 1906–1914.
- (23) Caruso, F.; Niikura, K.; Furlong, D. N.; Okahata, Y. *Langmuir* **1997**, *13*, 3422–3426.
- (24) Laurent, D.; Schlenoff, J. B. *Langmuir* **1997**, *13*, 1552–1557.
- (25) Debreczeny, M.; Ball, V.; Boulmedais, F.; Szalontait, B.; Voegel, J. C.; Schaaf, P. *J. Phys. Chem. B* **2003**, *107*, 12734–12739.
- (26) Boulmedais, F.; Schwinte, P.; Gergely, C.; Voegel, J. C.; Schaaf, P. *Langmuir* **2002**, *18*, 4523–4525.
- (27) Boulmedais, F.; Bozonnet, M.; Schwinte, P.; Voegel, J. C.; Schaaf, P. *Langmuir* **2003**, *19*, 9873–9882.
- (28) Griebenow, K.; Santos, A. M.; Carrasquillo, K. G. *Internet J. Vib. Spectrosc.* **1999**, *3*, edition 1.
- (29) Zhou, Y.; Wu, S.; Conticello, V. P. *Biomacromolecules* **2001**, *2*, 111–125.
- (30) Chehin, R.; Lloro, I.; Marcos, M. J.; Villar, E.; Shnyrov, V. L.; Arrondo, J. L. R. *Biochemistry* **1999**, *38*, 1525–1530.
- (31) Müller, M.; Kessler, B.; Lunkwitz, K. *J. Phys. Chem. B* **2003**, *107*, 8189–8197.
- (32) Greenfield, N. J. *Anal. Biochem.* **1996**, *235*, 1–10.
- (33) Beychok, S. In *Poly- α -amino Acid: Protein Models for Conformational Studies*; Fasman, G. D., Ed.; Marcel Dekker: New York, 1968.
- (34) Jiang, S.; Liu, M. *J. Phys. Chem. B* **2004**, *108*, 2880–2884.
- (35) Zhang, L.; Yuan, J.; Liu, M. *J. Phys. Chem. B* **2003**, *107*, 12768–12773.
- (36) Wang, Y.; Chang, Y. C. *Macromolecules* **2003**, *36*, 6503–6510, 6511–6518.
- (37) Vermonden, T.; Giacomelli, C. E.; Norde, W. *Langmuir* **2001**, *17*, 3734–3740.
- (38) Sreerama, N.; Woody, R. W. *Anal. Biochem.* **2000**, *282*, 252–260 and references therein.
- (39) Sauerbrey, G. Z. *Z. Phys.* **1959**, *155*, 206–222.
- (40) Rosenheck, K.; Doty, P. *Proc. Natl. Acad. Sci. U.S.A.* **1961**, *47*, 1775–1785.
- (41) Haynie, D.; Freire, E. *Proteins* **1993**, *16*, 115–140.
- (42) Yang, J.; Buck, M.; Pitkeathly, M.; Kotik, M.; Haynie, D.; Dobson, C.; Radford, S. *J. Mol. Biol.* **1995**, *252*, 483–491.
- (43) Morozova-Roche, L.; Arico-Muendel, C.; Haynie, D.; Emelyanenko, V.; Van Dael, H.; Dobson, C. *J. Mol. Biol.* **1997**, *268*, 903–921.
- (44) Cantor, C. R.; Timasheff, S. N. In *The Proteins*, 3rd ed.; Neurath, H., Hill, R. L., Eds.; Academic: New York, 1982; Vol. 5, pp 145–306.
- (45) Greenfield, N.; Fasman, G. D. *Biochemistry* **1969**, *8*, 4108–4115.
- (46) Alder, A. J.; Greenfield, N. J.; Fasman, G. D. *Methods Enzymol.* **1973**, *27*, 675–735.
- (47) Lvov, Y. In *Protein architecture, Interfacing Molecular Assemblies and Immobilization Biotechnology*; Lvov, Y., Möhwald, H., Eds.; Marcel Dekker: New York, 1999; pp 125–167.
- (48) Xie, A. F.; Granick, S. *J. Am. Chem. Soc.* **2001**, *123*, 3175–3176.
- (49) Picart, C.; Mutterer, J.; Richert, L.; Luo, Y.; Prestwich, G. D.; Schaaf, P.; Voegel, J. C.; Laval, P. *Proc. Natl. Acad. Sci. U.S.A.* **2002**, *99*, 12531–12535.
- (50) Laval, Ph.; Gergely, C.; Cuisinier, F. J. G.; Decher, G.; Schaaf, P.; Voegel, J. C.; Picart, C. *Macromolecules* **2002**, *35*, 4458–4465.

MA049136Y